Title

Conservation and host-specific expression of non-tandemly repeated heterogenous ribosome RNA gene in arbuscular mycorrhizal fungi

Running title

Conservation and expression of mycorrhizal rDNA

Authors

Taro Maeda*[1], Yuuki Kobayashi[1], Tomomi Nakagawa[1], Tatsuhiro Ezawa[2], Katsushi Yamaguchi[3], Takahiro Bino[3], Yuki Nishimoto[3], Shuji Shigenobu[3] & Masayoshi Kawaguchi*[1]

Affiliation

1 Division of Symbiotic Systems, National Institute for Basic Biology, Nishigonaka 38, Myodaiji, Okazaki, Aichi, Japan

2 Graduate School of Agriculture, Hokkaido University, Sapporo, Japan

3 Functional Genomics Facility, National Institute for Basic Biology, Nishigonaka 38, Myodaiji, Okazaki, Aichi, Japan

*Corresponding author

25 Email addresses:

26 TM: maedat@nibb.ac.jp

27 YK: kobayasi@nibb.ac.jp

28 TN: nkgwtmm@nibb.ac.jp

29 TE: tatsu@res.agr.hokudai.ac.jp

30 KY: kyamaguc@nibb.ac.jp

31 TB: bino@nibb.ac.jp

32 YN: nynishi@nibb.ac.jp

33 SS: shige@nibb.ac.jp

34 MK: masayosi@nibb.ac.jp

35

Abstract

The ribosomal RNA-encoding gene (rDNA) has a characteristic genomic nature: tens to thousands of copies in a genome, tandemly repeated structure, and intragenomic sequence homogeneity. These features contribute to ribosome productivity via physiological and evolutionary processes. We reported previously the exceptional absence of these features in the model arbuscular mycorrhizal (AM) fungus *Rhizophagus irregularis*. Here we examine the phylogenetic distribution of the exceptional rDNA features in the genus *Rhizophagus* via improving the genome sequence of *R. clarus*. Cross-species comparison indicated similarity of their rDNAs not only in the genomic features but also in the distribution of intragenomic polymorphic sites on the paralogs. Ribosomal RNA comprises multiple domains with different functions. The two *Rhizophagus* species commonly exhibited a variation enrichment site, ES27L, which is related to translational fidelity and antibiotic sensitivity. Variation enrichment on ES27L has not been observed in other organisms lacking the three rDNA features such as malaria parasites and *Cyanidioschyzon merolae*. Expression profiling of rDNAs in *R. irregularis* revealed that rDNA paralogs are expressed differently in association with host plant species. Our results suggest a broad distribution of the disarranged rDNA across AM fungi and its involvement in the successful association with the broad range of host species.

Introduction

Ribosome heterogeneity was first proposed by Francis Crick as the "one gene–one ribosome–one protein" hypothesis in 1958 [1]. This hypothesis, where a different type of ribosome translates each protein, vacillated within a few years, and the idea that "all ribosomes are exactly the same" became prevalent [2]. However, recent evidence of heterogeneous ribosomes in various organisms (e.g., humans, mouse, yeast, *Arabidopsis*, fruit flies, zebrafish, and malaria parasites) rekindled the notion that ribosome is an additional regulatory layer of gene expression [2–4]. Although a number of studies have reported the correlation between tissue- and cell stage-specific phenotypes and specialized ribosomes, the detailed expression control mechanisms and evolutionary contributions of this heterogeneity remain ambiguous [2–4]. Notably, the importance and distribution of the heterogeneity of the ribosomal RNA (rRNA) remain an open question. The reliable sequencing and mutant/transformant construction of the 18S–5.8S–28S ribosomal RNA-encoding loci (48S rDNA) have been technically challenging due to their large copy number (CN) and tandem repetitive structure (TRS) [2].

In the previous genomic study of the 48S rDNA in the model arbuscular mycorrhizal (AM) fungus *Rhizophagus irregularis* DAOM-181602, we unexpectedly found (1) a small copy number (around ten copies), (2) the absence of TRS, (3) and intragenomic heterogeneity [5]. AM fungi belong to the subphylum Glomeromycotina [6] and form symbiotic associations with most land plants [7, 8], and to date, up to 300 species have been described [9]. The association was established in the early Devonian and contributed to plant terrestrialization via enhancing nutrient uptake [10, 11]. AM fungi colonize plant roots and construct extensive hyphal networks in the soil and deliver essential nutrients to the host plant. AM fungi show no apparent host specificity; they are capable of colonizing different plant

functional groups, that is, autotrophic and heterotrophic plants, and connect them via the underground mycelial networks in the field [12, 13].

According to the recent ideas for the physiological contribution of ribosome heterogeneity in eukaryotes [2–4], it is hypothesized that the ribosome polymorphisms in *R. irregularis* assist adaptation to diverse environments and facilitate a broad host range via translational modifications [5]. The absence of the TRS of rDNA may allow us to elucidate not only the evolutionary mechanisms underlying the conservation of the TRS in the majority of eukaryotes but also those for overcoming the difficulty in rDNA mutation/transformation construction. However, the unique features of AM fungal rDNA have only been discovered very recently [5, 14], and the extent of the features in the Glomeromycotina still remains unexplored. Although genome sequences have recently been published in several species, including *R. clarus*, *Glomus cerebriforme*, *R. diaphanous*, *Gigaspora rosea*, *G. margarita*, and *Claroideoglomus claroideum* [15–18], the genomic structure of rDNA has been unclear except in *R. irregularis*, which is due to, at least partially, the difficulty in constructing genome assemblies long enough for the analysis of the rDNA structure.

To examine the nature of AM fungal rDNA in greater detail, we improved the genome data of *R. clarus* HR1 and analyzed whether *R. clarus* HR1 shares the three rDNA features and polymorphic sites with *R. irregularis* via cross-species comparison. Subsequently, we performed PacBio circular consensus sequencing (CCS) [19], which generates accurate long-read sequences, for profiling the expression of different rDNA paralogs in association with the environmental condition.

Results

Improved *R. clarus* genome assembly indicates high similarity in rDNA genomic structure between *R. irregularis*

Here, we obtained an improved *R. clarus* genome assembly covering all of the 48S rDNA loci that were expected based on the read depth of coverage (**Fig. 1)**. The improved *R. clarus* rDNA resembled that of *R. irregularis*: it exhibited 11 copies, a non-tandemly repeated structure, and heterogeneity among the copies (**Fig. 1b**).

The total size of the *R. clarus* contigs was comparable with the estimated genome size, and the gene models covered almost all of the eukaryotic conserved gene sets. A total of 5,819,346 PacBio reads were generated, with an average length of 3.4 kb (**Supplementary Tables 1 and 2**). The assembling and the error correction resulted in a sequence dataset containing 147 Mbp (360 contigs, N50 = 1.30 Mbp, 31,233 genes) (**INSDC; BLAL01000001-BLAL01000360**). A BUSCO analysis revealed high coverage of the eukaryotic conserved gene set (95.1%, DB; eukaryota_odb9, **Supplementary Table 2**). *R. clarus* contained a telomeric region on the edge of multiple contigs as *R. irregularis* (7 in *R. irregularis* and 63 in *R. clarus*). The nucleotide sequence of telomeres was "TTAGGG," similar to that of the majority of fungi [20]. Although the nuclear phase remains unclear in AM fungi [21], our data informed us that the AM fungus has the usual telomeric region and suggested the minimum expected number of chromosomes.

Our *R. clarus* assembly shared the three exceptional rDNA features with *R. irregularis*. RNAmmer found 11 copies of the complete 45S rDNA cluster, which was composed of 18S rRNA, intergenic spacer region 1 (ITS1), 5.8S rRNA, ITS2, and 28S rDNAs (**Fig. 1a, Supplementary Data 1, Supplementary Figure 1**). None of the *R. clarus* rDNAs formed the

TRS, comprising multiple tandemly repeated units of the 45S rDNAs. Most of the 45S clusters were located on different contigs; a single copy of rDNA was detected in three contigs, and two copies were found in four contigs (Fig. 1a). In cases in which two rDNA clusters were found, the two copies resided apart from each other and did not form a tandem repeat. The internal regions contained protein-coding genes, respectively, and the two clusters were located on reverse strands from each other. Because all rDNA copies were located >10 kb away from the edge of each contig (**Fig. 1a**), the absence of TRS was unlikely to be an artifact derived from an assembly problem. We found no synteny between the two *Rhizophagus* rDNAs.

To confirm that no rDNA clusters were overlooked, we estimated the rDNA CN based on the read depth of coverage. The mapping of the genomic Illumina reads onto the selected reference sequences indicated that the average coverage depth of the consensus rDNA was approximately nine times deeper than that of the genome, suggesting that *R. clarus* possesses around nine copies of rDNAs in its genome (**Fig. 1b, Supplementary Data 2**). Thus, we considered that our genome assembly (containing 11 rDNA copies) covered almost all of the rDNA copies.

The obtained rDNAs indicated polymorphism among the 45S rDNA clusters on *R. clarus*, similar to that of *R. irregularis*. Pairwise comparisons of the 11 rDNA copies detected an average of 40.9 indels and 76.8 sequence variants, whereas one of the sequence pairs (RCL_c3122_1 and RCL_c3122_2) had identical sequences (**Supplementary Data 3**).

To examine the phylogenetic distribution of the heterogeneous rDNAs, we constructed a phylogenetic tree with previously released *Rhizophagus* ITS sequences (**Fig 1d**). Before the phylogenetic analysis, we improved the erroneous region on the previous PacBio-based *R. irregularis* genome (GCA_002897155.1) using Illumina reads. The previous genome, which was corrected on the GATK software [5], was improved via a standard correction software

for long-read-based assemblies, Pilon [22]. The new assemblies obtained differed from the previous genome at 3,660,534 positions (2.4% of the alignment, **INSDC; BDIQ02000001-BDIQ02000210**). However, the ten 48S rDNA clusters exhibited no differences compared with the previous genomes. We used these rDNA regions as reference sequences hereafter. Phylogenetic analysis revealed that the rDNA polymorphisms of our *R. clarus* genome covered most of the polymorphisms reported previously for this species. Moreover, an rDNA cluster, RCL_c3086_1, established a clade with the *Rhizophagus cactus* rDNA (**Fig 1d**).

Distribution of non-tandemly repeated rDNAs across AM fungi

We researched the extensive conservation of the *Rhizophagus*-type rDNA using previously released fungal genomes. We selected four AM fungi and 20 non-AM fungal species from the public database and obtained successive results from two AM fungi and five non-AM species (**Supplementary Data 2**). The read depth and direct search of rDNA regions showed the conservation of the copy number reduction (CNR) and the TRS-lacking features among AM fungi. In the non-AM fungi, we obtained no evidence of the presence of the *Rhizophagus*-type rDNA.

To estimate rDNA copy number variation (CNV), we compared the abundance of Illumina reads aligned to rDNA and genomic sequences [23]. Due to the difficulty of the rDNA region assembling, we presumed that the read depth gives a more reliable estimation of the rDNA CNV than does the homology-based search of the assemblies. The estimated number of 48S rDNA copies was 1 or 10 in AM species (*G. cerebriforme* and *D. epigaea*) and 71–496 in the non-AM fungi (**Fig. 2, Supplementary Data 2**). These results suggest that the CNR is not limited to the genus *Rhizophagus* but is seemingly common among AM species. In non-AM species, we found no CN under 20 (**Fig. 2)**, which is lethal for yeast [24]. Even if we included the six species that contained a single or partial rDNA gene (see Material

and Methods, **Supplementary Data 2, Supplementary Figure 2**) in the analysis, no species contained over 20 rDNA copies, with the exception of *Jimgerdemannia flammicorona* (*Endogonales*; estimated CN, 2), which is a plant-symbiotic species [25].

Our searching of the rDNA regions on the public assemblies supported the absence of the TRS in the two AM species (*G. cerebriforme* and *D. epigaea*). The *D. epigaea* genome (GCA_003547095) had seven 48S rDNA clusters and two 28S rDNAs (**Fig. 2**). The depth-based CN, i.e., ten copies, suggested that the public genome contains the majority of the rDNA copies in *D. epigaea*. We cannot deny the possibility that the two 28S copies, which were located near the edge of contigs (1,760 bp and 522 bp), are part of the TRS structure. However, the depth-based CN suggests that even if the two 28S built the TRS on the inter-assembly region, these overlooked TRS would be short (under three copies). Another AM fungus, *G. cerebriforme* (GCA_003550305), had two clusters of 45S rDNA on the different contigs. Although these clusters were located near the edge of the contigs (1–3, 178 bp), the depth-based CN (one copy) denied the presence of a long TRS structure on the genome (**Fig. 2, Supplementary Data 2**).

In the five non-AM species, we obtained no evidence of the TRS-lacking feature. The public assemblies contained only part of the rDNA regions at 2–15 copies, and the rDNAs were located on the edge of assemblies (**Fig. 2**, **Supplementary Data 2**). Interestingly, two *Mucorales* species (*Phycomyces blakesleeanus* and *Mucor circinelloides*) contained one 45S rDNA located >10 kb away from the edge of the assembly (**Fig. 2**), respectively. Although the depth-based CN (*P. blakesleeanus*, 147–151 copies; *M. circinelloides*, 124–127 copies) indicated that the public genome data did not contain the majority of the rDNA regions, we found at least one TRS-lacking rDNA on this genome (**Fig. 2**). In an *Endogonaceae* species, *J. flammicorona*, the public genome had only one 28S rDNA. Although the read depth analysis

197 indicated the presence of a *Rhizophagus*-like CNR in this species, the public assemblies were
198 not sufficient to assess the genomic structure.

199 Regarding the intragenomic heterogeneity of the rDNA, the public genomes contained
200 too many ambiguous sites to allow a discussion of the heterogeneity. Hence, we skipped the
201 analysis of the intragenomic heterogeneity in the non-*Rhizophagus* group.

202 Distribution of intragenomic polymorphisms is highly similar
203 between the two *Rhizophagus* species

204 We then focused on the conservation of the intragenomic polymorphic site among the
205 AM species. A previous study of *R. irregularis* reported that the intragenomic polymorphic
206 site is not distributed uniformly on the rDNAs and argued that the variation-enriched site may
207 be upon the diversifying selection [5]. However, a report of a single species is insufficient to
208 exclude the possibility of the accumulation of random mutations at that site. Hence, we
209 compared the intragenomic polymorphic site between the two *Rhizophagus* species, and
210 found a similarity of the polymorphic site distribution. The variation-enriched site
211 corresponded with the yeast ES27L, which is one of the eukaryote-specific (ES) expansion
212 segments related to translation fidelity and antibiotic sensitivity [26–28].

213 To quantify the intragenomic polymorphism, we calculated the intragenomic
214 polymorphic sites for each 50-base window on the aligned rDNA copies. As references, we
215 selected *C. merolae* and a malaria parasite species, *Plasmodium falciparum*, due to the
216 similarity of their rDNA structure with that of AM fungi [29, 30]. The overview of the
217 polymorphism distribution was highly similar between *R. irregularis* and *R. clarus*, although
218 the remaining two species indicated several different patterns with them (**Fig. 3**). Many of the
219 variations were located on the ITS regions in all samples. The AM species and *P. falciparum*
220 had an additional peak on the forward region of 28S. The two AM fungi shared another peak

in the middle of the 28S rDNA. We then identified the corresponding region with the six domains on the *S. cerevisiae* 28S rDNA [31] via alignment, and revealed that the variation-enriched region in the AM fungi corresponded with domains I, III, IV, and VI. Intriguingly, the ES27L site of domain IV exhibited an especially high variation in both species (**Fig. 3**).

To assess the effect of the polymorphism on the rRNA secondary structure, we performed an *in silico* structure prediction. Before the prediction, we clustered the rDNA copies that had identical "domain IV" sequences and obtained five *R. irregularis* clusters and four *R. clarus* clusters (**Fig. 4a**). Our *in silico* analysis predicted that the AM fungi have three types of the "ES27L" structure; i.e., a *S. cerevisiae*-like structure (named yeast type), a "c" arm-lacking structure (straight type), and a structure with an additional branch on the "b" arm (beak type) (Fig. 4B). Although the beak type was only found in *R. clarus* (c3086-1), the yeast type and straight type were detected in the rDNA of both species. The yeast type was abundant in *R. irregularis* (eight in *R. irregularis* and two in *R. clarus*), and the straight type was more frequent in *R. clarus* (eight in *R. clarus* and two in *R. irregularis*). The phylogenetic analysis of the whole 28S rDNA sequences revealed that the copies that had the same structural type did not establish a monophyletic clade (**Fig. 4b**).

Host-specific rDNA expression in *R. irregularis*

To examine whether the rDNA expression profiles were affected by host conditions or the host species, we performed a PacBio CCS, which generates accurate long-read sequences through multiple repetitions of the sequencing of the same DNA molecules [19]. This method has been adopted in several ecological studies targeting rDNA in AM species [32, 33]. Our rRNA-targeting CCS showed that the rDNA expression profiles largely depended on the host plant species.

We constructed 23 CCS libraries from *R. irregularis*-colonizing plant organs (**Supplementary Data 4) (INSDC; PRJDB9672**). As a host plant, we used the model legume *Lotus japonicus* MG20 [34, 35] (17 libraries) and the basal land plant *Marchantia paleacea* [36] (6 libraries). We cultivated

246 the legume-infecting samples under five conditions (**Supplementary Data 4**) to analyze the
247 expression profiles after cuttings off the host shoots. The shoots cutting promotes the sporulation of
248 AM fungi [37]. We obtained 61,290 AM fugal reads from the libraries and clustered the CCS reads to
249 calculated the relative amount of each rRNA type. After several rounds of optimization of the CD-Hit-
250 est-2D [38] parameters, we obtained the best clustering of the sequences with -c 99.

251 The identified profiles showed a conserved rRNA expression ratio in *L. japonicus* mycorrhizal
252 roots with or without the shoot-cutting step in the host plants. Conversely, we detected significant
253 differences in their expression profiles between *L. japonicus* roots and *M. paleacea* thalli (**Fig. 5**). The
254 trend of the profiles was similar in types [c62_1, c62_2], [c312_1], [c356_1], and [c4_1]. However, it
255 was different in the remaining three types ([c35_1], [c39_1], and [c52_1, c311_1]), which exhibited
256 different rankings in the degree of expression according to the cultivation condition (**Fig. 5A**). The
257 PCA analysis of the rRNA profiles revealed that samples of colonized *L. japonicus* roots were
258 indistinguishable under the various conditions and that the clear distinction of profiles depended on
259 the host species (**Fig. 5b**). The multivariate analysis of variance (MANOVA) identified statistically
260 significant differences in the profiles ($P < 0.001$) (**Fig. 5b**).
261

Discussion

Here, we revealed that the three rDNA features of *R. irregularis* were conserved in *R. clarus* [5, 14], i.e., (1) decreased copy count of the 48S rDNA, (2) absence of the TRS, and (3) intragenomic heterogeneity. Moreover, our analysis of the public genome data supported the wide distribution of the disarranged rDNA (a handful of TRS-lacking rDNAs) in non-*Rhizophagus* AM fungi. The cross-species comparison found conservation of the variation-enriched sites, ES27L, between *R. irregularis* and *R. clarus*. The rRNA-targeting clustering showed that the rRNA expression profiles were affected by the host plant species.

Based on the improved/reanalyzed genome data, we found that three AM species commonly had an exceptionally low 48S rDNA CN (*R. clarus*, 11 copies; *G. cerebriforme*, 2 copies; and *D. epigaea*, 7–10 copies). The previously reported CN in *R. irregularis* (ten copies) was the lowest among eukaryotes other than pneumonia-causing *Pneumocystis* (one copy) [39], *C. merolae* (three copies) [29], and malaria-causing *Plasmodium* (five to eight copies) [5, 30]. The CNV of the rDNA ranged from 14 to 1,442 in other fungi [23]. The rDNA CN is relevant for translation efficiency, because multiple rDNAs are required to synthesize a sufficient amount of rRNA [24, 40]. Although an rDNA CN <20 is lethal in *S. cerevisiae* [24], the successive cultivation of AM fungi with their reduced rDNA counts suggested that the handful of rDNA copies is sufficient to support the growth of AM fungi. Our team previously hypothesized that the AM fungus has a unique ribosome synthesis step to recover from the low rDNA CN, based on the results obtained for a single AM species, *R. irregularis* [5]. The conservation of the rDNA CNR identified here supports the generalization of our previous hypothesis to the genus *Rhizophagus* and the AM fungus.

Our depth-based CNV analysis of non-AM fungi suggested that a sister group of the AM fungus, *Mucorales*, retained the ordinary number of rDNA copies (71–151) (**Fig. 2, Supplementary Data 2**). The simple mapping to the phylogenetic tree indicated that the

CNR occurred on the common ancestor of the AM fungus, although rDNA data for *Endogonales* (a plant-symbiotic group closely related to *Mucorales*) [25] have not been collected (**Supplementary Figure 2**). It is interesting that a previous study identified CNR on distantly related plant-symbiotic fungi (e.g., *Oidiodendron maius*, 11 copies; *Phialocephala scopiformis*, 15 copies; *Cenococcum geophilum*, 15 copies; and *Meliniomyces variabilis*, 18 copies) [23]. Although the genomic structure and intragenomic heterogeneity of these species remain unknown, the rDNA CNR may be a universal trend related to plant root symbiosis.

We also found evidence of the conservation of the absence of the TRS in AM fungi. The TRS-lacking feature has been observed only in the *R. irregularis*, malaria parasites, and *C. merolae* genomes, which exhibit 48S rDNA CNR (malaria parasites, five to eight copies; *C. merolae*, three copies). This correspondence between the TRS-lacking and CNR features is reasonable because the TRS is part of the recovery system of the rDNA CN, i.e., unequal sister chromatid recombination (USCR) [41]. The TRS increases the rDNA CN via recombination with a neighbor repeat during the DNA duplication stages [42]. An unknown highly efficient rRNA synthesis activity in the AM fungus might reduce the selective pressure against the retention of the rDNA CN and might disrupt the TRS in AM fungi. We found both TRS-lacking and TRS-keeping 48S rDNAs in the two *Mucorales* species (**Fig. 2**). Although the genomic structure of the remaining rDNA copies in these species is unclear, the TRS-lacking rDNA might have arisen from a normal TRS-containing rDNA in the common ancestor of the AM fungus and *Mucorales*; subsequently, the ancestral AM fungus might have lost the TRA-containing rDNAs.

The heterogeneity of the intragenomic sequence in rDNA is attractive in terms of ribosome heterogeneity. The evolutional model of the rDNA has assumed that the TRS-dependent CN recovery causes the homogeneity of the rDNA through the bottleneck effect (concerted evolution) [24]. Several organisms, including the TRS-lacking malaria parasites,

312 exhibit rDNA/rRNA heterogeneity with tissue- and cell stage-specific expression patterns
313 [43–45]. However, the functional consequences of this rRNA variation have not been
314 established [2], and It was also unclear whether the rDNA heterogeneity is related with an
315 adaptation or an evolutionarily neutral diversification. We revealed the conservation of
316 polymorphism-enriched region of ITS, domains I, III, IV, and VI, between the two
317 *Rhizophagus* (**Fig. 3**). For the ITS region, a similar variation accumulation was determined
318 from other TRS-lacking species (*C. merolae* and *P. falciparum*). This accumulation may be
319 attributed to their weak evolutional constraints compared with rRNA-encoding regions.
320 Conversely, the variation peak on the ES27L site of domain IV was only found on the two
321 AM fungi; the polymorphism of *C. merolae* was very weak on the rRNA-encoded region, and
322 *P. falciparum* exhibited a scattered distribution of the variation site for all RNA-encoded
323 regions (**Fig. 3**). The data concerning *C. merolae* indicate that the polymorphism on ES27L is
324 not inevitable in TRS-lacking eukaryotes. These results suggest that the polymorphisms did
325 not occur randomly on the AM rDNAs, but they reflected some functional redundancy or
326 disruptive selection on the region. Specific alleles on this site may be maintained for
327 unknown evolutional reasons.

328 Our *in silico* secondary structure analysis indicated that intragenomic variations were
329 scattered over the “b” stem loops of *Rhizophagus* ES27L (**Fig. 4**). Moreover, the two AM
330 fungi commonly had an rDNA genotype lacking the “c” arm (straight type). In multiple
331 species, the ES27L has been modeled in cryo-EM, to point toward the peptide exit tunnel of
332 the ribosome [46, 47]. A previous experimental deletion indicated that the “b” arm has a
333 function in translation fidelity via binding to methionine aminopeptidase (MAP1) in *S.*
334 *cerevisiae*; the deletions in the “b” arm induce amino acid misincorporation and stop codon
335 read through upon treatment with translational-error-inducing antibiotics (paromomycin) [27],
336 and the whole deletion of “b” changes the proteomic profiles [28]. The polymorphism

337 observed on the AM fungal “b” arm may contribute to translation fidelity control and
338 modulates the sensitivity against antibiotics. The heterogeneity observed in ES27L was not
339 accompanied by the diversification of the binding protein on the platform; two *Rhizophagus*
340 genomes contained the single ortholog of yeast Map1, respectively (Supplementary Data 6). It
341 should be noted that the deletions in the “b” arm increased the resistance against anisomycin
342 and cycloheximide in yeast [27], indicating that the complete “b” arm reduces the resistance
343 against these antibiotics. This trade-off might result in the selection of the diversification of
344 the AM fungal rDNA. It should be noted that plants have an antibiotic-like substrate that is
345 used for self-defense [48]. For example, ricin from *Ricinus communis* cleaves the *N*-
346 glycosidic bond in 28S rRNA [49]. The intragenomic diversity of rDNA may enable
347 symbionts to pass through the species-specific diversified defense mechanisms of plants and
348 contribute to the establishment of symbiosis with a broad range of plant species.

349 Regarding the “c” arm, the deleted yeast did not display any changes in the sensitivity
350 or tolerance to any of the inhibitors tested (cycloheximide, anisomycin, and hygromycin B)
351 [27]. However, the conservation of the “c” arm among eukaryotes suggests their importance
352 for life. The deletion of the whole ES27L is lethal in yeast and *Tetrahymena* [26, 50].
353 Meanwhile, in *Drosophila* ribosomes, the interaction between the “c arm” and the S8e
354 ribosomal protein forms an intersubunit bridge and was considered to contribute to the
355 conformation dynamics of the binding with the elongation factor 2 (eEF2) [51]. Nonetheless,
356 future studies of the effect against various antibiotics are needed to reveal the function of
357 ES27L in AM species.

358 The heterogeneity of the rDNA is also an important subject in terms of biodiversity.
359 Our *R. clarus* genome assembly indicated that intragenomic variation covered most of the
360 polymorphisms previously reported in this species (**Fig. 1d**). This result provides an incentive
361 to review the rDNA diversity of other AM fungi. The ITS and a part of the 28S rDNA have

been widely used as a marker gene for the ecological and taxonomic studies of AM fungi [52]. The intraindividual rDNA diversity of AM fungi has been indicated because multiple rDNA genotypes were reported from the single fungal body in many AM species [53–57]. Single-nucleus sequencing indicated that this multinucleate fungus has genetically different nuclei in its body (heterokaryosis) [14, 15, 58]. Our previous finding of intragenomic heterogeneity in *R. irregularis* led to a discussion of the contribution of the combination of heterokaryosis and intragenomic heterogeneity to intraindividual heterogeneity within a fungal body [5]. The present results from *R. clarus* reinforce the hypothesis that the multilayered diversification mechanism causes intraindividual rDNA heterogeneity in *Rhizophagus*. The intragenomic variation in *R. irregularis* was not sufficient to disrupt species-level identification [5]. However, our result that an *R. clarus* rDNA copy established a clade with the sequence of *R. cactus* (**Fig. 1d**) indicated that imbalanced amplification and sequencing among the paralogs have the potential to cause erroneous identification of species.

The rRNA profile of *R. irregularis* identified here was similar under the same incubation condition but was modified by drastic changes in the condition. A previous RNA-seq study indicated that all of the rDNA genotypes retained the translation activity in a pre-infected stage of *R. irregularis* [5]. The rRNA profiles were significantly affected by the variation of the incubation period (22–36 dpi and 3 months) and the type of host plant (legumes to liverworts). Moreover, the ratio of each rRNA type was not correlated with the CN of each rDNA gene (**Fig. 5**). Due to the slow growth rate of liverwort-infected AM fungi, we cannot align the incubation period with that of the legume-infected sample. However, the observed dynamics suggest that the AM fungus changed the 28S rDNA expression of each copy via a yet unknown environment-specific expression control system. Other species containing heterogeneous rDNA/rRNA (malaria parasites, zebrafish, mice, and humans) [43, 44, 51, 59] also exhibit similar condition-dependent expression changes. Although these

387 organisms have complete replacements of the rRNA type at some developmental stages [59],
388 we found no replacement of the rRNA types under the adopted conditions. We used the whole
389 body of the incubated AM fungi together with host plant roots. Additional structure-specific
390 rRNA sampling would provide insights into the dynamics and their adaptive contribution to
391 AM fungi. The principal component score and the actual change in the reading count ratio
392 indicated that the change of [c52_1, c311_1]-type expression ratio relates to the host-
393 dependent modification. Interestingly, the [c52_1, c311_1] type lacks the "c" arm on the
394 ES27L, and some SNP on "b" arms were determined based on a comparison with the
395 remaining types (**Fig. 4**). This result tempted us to speculate that this [c52_1, c311_1]-derived
396 rRNA affords a suitable ribosome for the symbiosis with liverworts.

397 Here, we indicated the possibility of relationships between plant symbiosis and
398 disarranged heterogeneous rDNA. Although multiple genomes of mutualistic eukaryote have
399 been identified [60]. Extended genomes: symbiosis and evolution), the previous studies
400 ignored the analysis of rDNA due to the difficulty in assembling their genome. The
401 assumption that all the eukaryotes have homogeneous TRS-making rDNAs may have drawn
402 attention away from rDNA diversity. The recent "renaissance" of ribosome heterogeneity [2]
403 may renew the study not only of embryology/physiology but also of symbiotic biology.
404

Material and Methods

PacBio-based genome assembling

The genome sequencing and gene annotation of *R. clarus* HR1 (MAFF:520076) was performed according to a previous study [5], with some modification (Supplementary Data 9). We isolated a complete mitochondrial sequence from the contigs and then submitted the assemblies to the DDBJ (nuclear DNA = BLAL01, mitochondrial DNA = LC506577). For the prompt submission of the genomic gene model data to DDBJ, we used GFF2MSS ver. 3.0.2 script (https://github.com/maedat/GFF2MSS).

Detection of ribosomal DNA and intragenomic polymorphisms

Ribosomal DNA regions were detected by RNAmmer ver. 1.284 [61]. In *R. clarus*, the RNAmmer-based regions were refined manually based on the MAFFT v7.429-based [62] alignment to the 48S rRNA of *S. cerevisiae* S288C. The genomic positions of rDNAs were visualized using our script, GeneHere version 0.1.1 (https://github.com/maedat/GeneHere). The species analyzed and genomic data are summarized in **Supplementary Data 2**. We adopted the rDNA searches against 26 species and obtained multiple 18S and 28S sequences from 12 species. We excluded the remaining samples containing only a part of the 48S rDNA sequence from the downstream analysis.

The number of rDNA paralogs was estimated based on the mean depth of coverage. From public short-read data, we found suitable data for nine species (**Supplementary Data 2**). The obtained read data were mapped to the references (whole-genomic data, extracted 18S, or 28S rDNA sequences) using bowtie2 version 2.3.5.1. The coverage depth of the references was calculated using bedtools version v2.29.0 (bedtools genomecov command with -d option),

and the statistics of each region were calculated and visualized using the R software ver. 3.6.1 with the ggplot2 ver. 3.2.1 package.

The difference among the rDNA paralogs was calculated using our script, AliVa (https://github.com/maedat/AliVa), and the sequences were aligned by MAFFT ver. 7.427 (options: --auto). The neighbor-net tree presented in **Fig. 1b** was generated by SplitsTree4 ver. 4.14.8 (raw sequence data: 10.6084/m9.figshare.11880780) [63]. The phylogenetic trees depicted in Fig. 1c were constructed based on the MAFFT alignment (10.6084/m9.figshare.11880834) using the ML method with IQ-TREE ver.1.6.11 (options: -nt AUTO) [64]; they were also tested for robustness by bootstrapping (1000 pseudoreplicates).

Analysis of the secondary structure of rDNA

The secondary structure of the *Rhizophagus* 28S rDNAs was predicted in silico. Domains I–VI were determined through the manual alignment with the *S. cerevisiae* 28S rDNA. We then cut out each domain from the *Rhizophagus* rDNAs and predicted the secondary structure of each domain. We used RNAstructure ver. 6.1 for structure prediction and StructureEditor ver 6.1 for visualization [65]. After the prediction of the top five minimum free energy structures, we chose the structure that exhibited the greatest similarity to that of *S. cerevisiae*.

Expression dynamics of rRNA

The expression levels of the rDNA paralogs were examined with PacBio sequel in total RNA extracted from plant-infected *R. irregularis* DAOM-181602. Thalli of *Marchantia paleacea* subsp. *diptera* were grown with *R. irregularis* DAOM-181602 (Premier Tech) in growth conditions, as described previously [36].

449 Total RNAs were isolated using the modified CTAB method, as described
450 previously by Nakagawa et al. (2011) [66], with some modifications (Supplementary Data 9).
451 *Lotus japonicus* MG-20 seeds were surface sterilized and germinated on an agar plate
452 containing no nutrients. Plants were grown in an artificially lit growth cabinet at 24°C for 16
453 h (light) and 22°C for 8 h (dark). After 6 days, the seedlings were transferred to soil, as
454 described previously by Miyata et al. (2014), with or without spores of *R. irregularis*. After
455 22 days, some of these plants were cut, their aerial parts were removed, and plants were
456 harvested at 2, 6, or 14 days after shoot removal.

457 The library used for PacBio CCS was prepared according to the protocol "Full-
458 Length 16S Amplification, SMRTbell Library Preparation and Sequencing" (Pacific
459 Biosciences, Part Number 101-599-700 version 01), with some modifications (Supplementary
460 Data 9). The CCS sequences were generated on a PacBio Sequel sequencer using a Sequel
461 Binding and Internal Control Kit 3.0 Mag Bead Binding Buffer Kit v2, and Sequel
462 Sequencing Kit 3.0 (Pacific Biosciences). The raw reads obtained were assembled using
463 SMRTLINK7 (Pacific Biosciences).
464

Author contributions

TM and MK conceived of and designed the experiments; TM, YK, TE, KY, TB, YN, SS, and MK performed the *R. clarus* genomic experiments and analyses; TM, TN, KY, SS, and MK performed the *R. irregularis* transcriptomic experiments and analyses. TM, TN, TE, SS, MK wrote the paper.

Acknowledgment

This work was supported by JST ACCEL Grant Number JPMJAC1403 and MEXT/JSPS KAKENHI Grant Number 19K22269, Japan. We thank Miwako Matsumoto, the Functional Genomics Facility and the Data Integration and Analysis Facility at the National Institute for Basic Biology for technical support; Katsuharu Saito, Kohki Akiyama. Computations were partially performed on the NIG supercomputer at ROIS National Institute of Genetics.

Competing Interests:

The authors declare no competing financial interests.

Figure Legends

Fig. 1 Ribosomal DNAs of *R. clarus* and *R. irregularis*. **a** Genomic positions of the 48S rDNA clusters on the constructed contigs. Rir, *Rhizophagus irregularis* (cyan); Rcl, *Rhizophagus clarus* (magenta). Red and purple bar (with asterisk) indicate 48S rDNA, and telomeric region, respectively. Contigs with no 48S rDNA were omitted from the figure. **b** Read depth of coverage of the *R. clarus* rDNA regions and whole-genomic region. Red dots indicate mode value. **c** Neighbor-net tree based on the whole sequence of 48S rDNA sequences. **d** Maximum likelihood (ML) tree based on the ITS region of the rDNAs (420 positions) (raw data, https://doi.org/10.6084/m9.figshare.11880834, 10.6084/m9.figshare.12251768, 10.6084/m9.figshare.11880780)

Fig. 2 Predicted rDNA copy number and the distribution on the constructed genome data of the 18S and 28S rDNA. The colors are as in the left top box. The tree on the left was generated by the ML analysis of 96 single-copy genes. The bold line indicates the node supported with 100 bootstrap value. The species analyzed are presented using the abbreviations (Rir, *R. irregularis*; Rcl, *R. clarus*; Gce, *G. cerebriforme*; Dep, *D. epigaea*; Sra, *Syncephalastrum racemosum*; Hve, *Hesseltinella vesiculosa*; Mci, *Mucor circinelloides*; Pbl, *P. blakesleeanus*; Pfi, *Piromyces finnis*). The central bar plot shows the predicted copy number of rDNA based on the read mapping back (bar) and actually observed number in the public genome (black dot and triangle). The right plot shows the positions of the determined rDNA on each public genome sequence. Red bar indicates 48S, 18S, or 28S rDNA-encoding region. The sub-boxes indicate the expanded view of a part of the plot. Raw values of the analysis are presented in Supplementary Data 2.

506 **Fig. 3** Distribution of rDNA sequence variants within the 48S rDNA. Numbers of 48S rDNA
507 in each species were described next to the right of the species name. The boxes above the x-
508 axis indicate the 18S-5.8S-28S ribosomal RNA-encoding region. The secondary structure of
509 the *S. cerevisiae* 28S rRNA was placed on the top right. The structure corresponding to
510 ES27L was highlighted in red and magnified in the sub-box.
511
512 **Fig. 4** Polymorphisms on the ES27L region of the 28S rDNA/RNA. **a** Alignment of ES27L
513 regions. The intragenomic conserved positions within each species were masked with gray
514 color. **b** Secondary structures obtained from the *in silico* prediction of domain IV. Magenta, *R.*
515 *clarus*; cyan, *R. irregularis*. The bottom ML tree was prepared from the whole 28S rDNA
516 sequence. The abbreviations are defined in Supplementary Data 2.
517
518 **Fig. 5** Expression profiles of the rDNA in *R. irregularis* colonizing different host species and
519 at different growth conditions. **a** Read count ratio in each AM fungal CCS library. Each point
520 indicates the value from a sample (error bar = standard deviation). The bar represents the
521 average of the values. The colors and point shapes indicate the type of rDNA. Legends are
522 provided in the right-bottom box. The x-axis represents the condition of the colonized root
523 samples of *L. japonicus* MG20 (CL-S). CL, shoot cutting at 22 days postinoculation (dpi) and
524 sampling at 36 dpi; CM, shoot cutting at 22 dpi and sampling at 28 dpi; CS, shoot cutting at
525 22 dpi and sampling at 24 dpi; L, cultivated for 36 dpi; S, cultivated for 24 dpi; MP,
526 inoculated in *M. paleacea* and cultivated for three months. **b** Biplot of the principal
527 component analysis (PCA) and their principal component score (red arrow). Each point
528 represent a sample. The shape and color of the points indicate the difference of host species
529 and growth conditions (see the top left box). Sample names were described to near the points.

References

1. Crick FH. On protein synthesis. *Symp Soc Exp Biol* 1958; **12**: 138–163.
2. Genuth NR, Barna M. The discovery of ribosome heterogeneity and its implications for gene regulation and organismal life. *Mol Cell* 2018; **71**: 364–374.
3. Dinman JD. Pathways to specialized ribosomes: the brussels lecture. *J Mol Biol* 2016; **428**: 2186–2194.
4. Xue SF, Barna M. Specialized ribosomes: a new frontier in gene regulation and organismal biology. *Nat Rev Mol Cell Biol* 2012; **13**: 355–369.
5. Maeda T, Kobayashi Y, Kameoka H, Okuma N, Takeda N, Yamaguchi K, et al. Evidence of non-tandemly repeated rDNAs and their intragenomic heterogeneity in *Rhizophagus irregularis.* *Commun Biol* 2018; **1**: 87.
6. Spatafora JW, Chang Y, Benny GL, Lazarus K, Smith ME, Berbee ML, et al. A phylum-level phylogenetic classification of zygomycete fungi based on genome-scale data. *Mycologia* 2016; **108**: 1028–1046.
7. Bonfante P, Genre A. Mechanisms underlying beneficial plant–fungus interactions in mycorrhizal symbiosis. *Nat Commun* 2010; **1**: 48.
8. Corradi N, Bonfante P. The arbuscular mycorrhizal symbiosis: origin and evolution of a beneficial plant infection. *PLoS Pathog* 2012; **8**.
9. Öpik M, Davison J. Uniting species- and community-oriented approaches to understand arbuscular mycorrhizal fungal diversity. *Fungal Ecology* . 2016. , **24**: 106–113
10. van der Heijden MGA, Klironomos JN, Ursic M, Moutoglis P, Streitwolf-Engel R, Boller T, et al. Mycorrhizal fungal diversity determines plant biodiversity, ecosystem variability and productivity. *Nature* 1998; **396**: 69–72.
11. Van Der Heijden MGA, Martin FM, Selosse M-A, Sanders IR. Mycorrhizal ecology and evolution: the past, the present, and the future. *New Phytol* 2015; **205**: 1406–1423.

12. Davison J, Moora M, Ouml;pik M, Adholeya A, Ainsaar L, Ba A, et al. Global assessment of arbuscular mycorrhizal fungus diversity reveals very low endemism. *Science* 2015; **349**: 970–973.
13. Gianinazzi-Pearson V. Plant cell responses to arbuscular mycorrhizal fungi: getting to the roots of the symbiosis. *Plant Cell* 1996; **8**: 1871–1883.
14. Lin K, Limpens E, Zhang Z, Ivanov S, Saunders DGO, Mu D, et al. Single nucleus genome sequencing reveals high similarity among nuclei of an endomycorrhizal fungus. *PLoS Genet* 2014; **10**: e1004078.
15. Montoliu-Nerin M, Sánchez-García M, Bergin C, Grabherr M, Ellis B, Kutschera VE, et al. Building *de novo* reference genome assemblies of complex eukaryotic microorganisms from single nuclei. *Sci Rep* 2020; **10**: 1303.
16. Morin E, Miyauchi S, San Clemente H, Chen ECH, Pelin A, de la Providencia I, et al. Comparative genomics of *Rhizophagus irregularis, R. cerebriforme, R. diaphanus* and *Gigaspora rosea* highlights specific genetic features in Glomeromycotina. *New Phytol* 2019; **222**: 1584–1598.
17. Venice F, Ghignone S, Salvioli di Fossalunga A, Amselem J, Novero M, Xianan X, et al. At the nexus of three kingdoms: the genome of the mycorrhizal fungus *Gigaspora margarita* provides insights into plant, endobacterial and fungal interactions. *Environ Microbiol* 2020; **22**: 122–141.
18. Kobayashi Y, Maeda T, Yamaguchi K, Kameoka H, Tanaka S, Ezawa T, et al. The genome of *Rhizophagus clarus* HR1 reveals a common genetic basis for auxotrophy among arbuscular mycorrhizal fungi. *BMC Genomics* 2018; **19**: 465.
19. Wenger AM, Peluso P, Rowell WJ, Chang P-C, Hall RJ, Concepcion GT, et al. Accurate circular consensus long-read sequencing improves variant detection and assembly of a human genome. *Nat Biotechnol* 2019; **37**: 1155–1162.
20. Cohn M, Liti G, Barton DBH. Telomeres in fungi. *Comparative Genomics*. 2005. Topics in current genetics, pp 101–130.
21. Kamel L, Keller-Pearson M, Roux C, Ané J-M. Biology and evolution of arbuscular mycorrhizal symbiosis in the light of genomics. *New Phytol* 2017; **213**: 531–536.

584 22. Walker BJ, Abeel T, Shea T, Priest M, Abouelliel A, Sakthikumar S, et al. Pilon: an integrated
585 tool for comprehensive microbial variant detection and genome assembly improvement. *PLoS*
586 *One* 2014; **9**: e112963.
587 23. Lofgren LA, Uehling JK, Branco S, Bruns TD, Martin F, Kennedy PG. Genome□based estimates
588 of fungal rDNA copy number variation across phylogenetic scales and ecological lifestyles. *Mol*
589 *Ecol* 2019; **28**: 721–730.
590 24. Ganley ARD, Kobayashi T. Highly efficient concerted evolution in the ribosomal DNA repeats:
591 Total rDNA repeat variation revealed by whole-genome shotgun sequence data. *Genome Res*
592 2007; **17**: 184–191.
593 25. Chang Y, Desirò A, Na H, Sandor L, Lipzen A, Clum A, et al. Phylogenomics of Endogonaceae
594 and evolution of mycorrhizas within Mucoromycota. *New Phytol* 2019; **222**: 511–525.
595 26. Ramesh M, Woolford JL Jr. Eukaryote-specific rRNA expansion segments function in ribosome
596 biogenesis. *RNA* 2016; **22**: 1153–1162.
597 27. Fujii K, Susanto TT, Saurabh S, Barna M. Decoding the function of expansion segments in
598 ribosomes. *Mol Cell* 2018; **72**: 1013–1020.e6.
599 28. Shankar V, Rauscher R, Reuther J, Gharib WH, Koch M, Polacek N. rRNA expansion segment
600 27Lb modulates the factor recruitment capacity of the yeast ribosome and shapes the proteome.
601 *Nucleic Acids Res* 2020.
602 29. Matsuzaki M, Misumi O, Shin-I T, Maruyama S, Takahara M, Miyagishima S-Y, et al. Genome
603 sequence of the ultrasmall unicellular red alga *Cyanidioschyzon merolae* 10D. *Nature* 2004; **428**:
604 653–657.
605 30. Gardner MJ, Hall N, Fung E, White O, Berriman M, Hyman RW, et al. Genome sequence of the
606 human malaria parasite Plasmodium falciparum. *Nature* 2002; **419**: 498–511.
607 31. Petrov AS, Bernier CR, Gulen B, Waterbury CC, Hershkovits E, Hsiao C, et al. Secondary
608 structures of rRNAs from all three domains of life. *PLoS One* 2014; **9**: e88222.
609 32. Schlaeppi K, Bender SF, Mascher F, Russo G, Patrignani A, Camenzind T, et al. High-resolution
610 community profiling of arbuscular mycorrhizal fungi. *New Phytol* 2016; **212**: 780–791.
611 33. Tedersoo L, Tooming-Klunderud A, Anslan S. PacBio metabarcoding of fungi and other

612 eukaryotes: errors, biases and perspectives. *New Phytol* 2018; **217**: 1370–1385.

613 34. Kawaguchi M. *Lotus japonicus* `miyakojima' mg-20: an early-flowering accession suitable for
614 indoor handling. *J Plant Res* 2000; **113**: 507–509.

615 35. Kato T, Kaneko T, Sato S, Nakamura Y, Tabata S. Complete structure of the chloroplast genome
616 of a legume, *Lotus japonicus*. *DNA Res* 2000; **7**: 323–330.

617 36. Kobae Y, Ohtomo R, Morimoto S, Sato D, Nakagawa T, Oka N, et al. Isolation of native
618 arbuscular mycorrhizal fungi within young thalli of the liverwort *Marchantia paleacea*. *Plants*
619 2019; **8**.

620 37. Redhead JF. Endotrophic mycorrhizas in Nigeria: some aspects of the ecology of the endotrophic
621 mycorrhizal association of *Khaya grandifoliola* C. DC. *Endomycorrhizas; Proceedings of a*
622 *Symposium* 1975.

623 38. Fu L, Niu B, Zhu Z, Wu S, Li W. CD-HIT: accelerated for clustering the next-generation
624 sequencing data. *Bioinformatics* 2012; **28**: 3150–3152.

625 39. Cushion MT, Keely SP. Assembly and annotation of *Pneumocystis jirovecii* from the human lung
626 microbiome. *MBio* 2013; **4**.

627 40. Milo R, Phillips R, Goodsell DS, Lane N, Nelson P, Hoffmann PM, et al. Cell biology by the
628 numbers. *Taylor & Francis Inc*. https://www.bookdepository.com/Cell-Biology-by-Numbers-
629 Ron-Milo/9780815345374. Accessed 5 Mar 2018.

630 41. Ganley ARD, Ide S, Saka K, Kobayashi T. The effect of replication initiation on gene
631 amplification in the rDNA and its relationship to aging. *Mol Cell* 2009; **35**: 683–693.

632 42. Kobayashi T. Ribosomal RNA gene repeats, their stability and cellular senescence. *Proceedings*
633 *of the Japan Academy Series B-Physical and Biological Sciences* 2014; **90**: 119–129.

634 43. Gunderson JH, Sogin ML, Wollett G, Hollingdale M, de la Cruz VF, Waters AP, et al.
635 Structurally distinct, stage-specific ribosomes occur in *Plasmodium*. *Science* 1987; **238**: 933–937.

636 44. Li J, Wirtz RA, McConkey GA, Sattabongkot J, McCutchan TF. Transition of *Plasmodium vivax*
637 ribosome types corresponds to sporozoite differentiation in the mosquito. *Mol Biochem Parasitol*
638 1994; **65**: 283–289.

639 45. Waters AP. The ribosomal RNA genes of *Plasmodium*. *Adv Parasitol* 1994; **34**: 33–79.

640 46. Armache J-P, Jarasch A, Anger AM, Villa E, Becker T, Bhushan S, et al. Cryo-EM structure and
641 rRNA model of a translating eukaryotic 80S ribosome at 5.5-A resolution. *Proc Natl Acad Sci U*
642 *S A* 2010; **107**: 19748–19753.
643 47. Greber BJ, Boehringer D, Montellese C, Ban N. Cryo-EM structures of Arx1 and maturation
644 factors Rei1 and Jjj1 bound to the 60S ribosomal subunit. *Nat Struct Mol Biol* 2012; **19**: 1228–
645 1233.
646 48. Savoia D. Plant-derived antimicrobial compounds: alternatives to antibiotics. *Future Microbiol*
647 2012; **7**: 979–990.
648 49. Endo Y, Tsurugi K. The RNA N-glycosidase activity of ricin A-chain. The characteristics of the
649 enzymatic activity of ricin A-chain with ribosomes and with rRNA. *J Biol Chem* 1988; **263**:
650 8735–8739.
651 50. Sweeney R, Chen L, Yao MC. An rRNA variable region has an evolutionarily conserved
652 essential role despite sequence divergence. *Mol Cell Biol* 1994; **14**: 4203–4215.
653 51. Parks MM, Kurylo CM, Dass RA, Bojmar L, Lyden D, Vincent CT, et al. Variant ribosomal
654 RNA alleles are conserved and exhibit tissue-specific expression. *Sci Adv* 2018; **4**: eaao0665.
655 52. Krishnamoorthy R, Premalatha N, Karthik M, Anandham R, Senthilkumar M, Gopal NO, et al.
656 Molecular markers for the identification and diversity analysis of arbuscular mycorrhizal fungi
657 (AMF). *Fungal Biology* . 2017. , 177–199
658 53. Sanders IR, Alt M, Groppe K, Boller T, Wiemken A. Identification of ribosomal DNA
659 polymorphisms among and within spores of the *Glomales*: application to studies on the genetic
660 diversity of arbuscular mycorrhizal fungal communities. *New Phytologist* . 1995. , **130**: 419–427
661 54. LloydMacgilp SA, Chambers SM, Dodd JC, Fitter AH, Walker C, Young JPW. Diversity of the
662 ribosomal internal transcribed spacers within and among isolates of *Glomus mosseae* and related
663 mycorrhizal fungi. *New Phytol* 1996; **133**: 103–111.
664 55. Hosny M, Hijri M, Passerieux E, Dulieu H. rDNA units are highly polymorphic in *Scutellospora*
665 *castanea* (Glomales, Zygomycetes). *Gene* 1999; **226**: 61–71.
666 56. Hijri M, Sanders IR. The arbuscular mycorrhizal fungus *Glomus intraradices* is haploid and has a
667 small genome size in the lower limit of eukaryotes. *Fungal Genet Biol* 2004; **41**: 253–261.

668 57. Pawlowska TE, Taylor JW. Organization of genetic variation in individuals of arbuscular
669 mycorrhizal fungi. *Nature* 2004; **427**: 733–737.
670 58. Chen ECH, Morin E, Beaudet D, Noel J, Yildirir G, Ndikumana S, et al. High intraspecific
671 genome diversity in the model arbuscular mycorrhizal symbiont *Rhizophagus irregularis. New*
672 *Phytol* 2018.
673 59. Locati MD, Pagano JFB, Girard G, Ensink WA, van Olst M, van Leeuwen S, et al. Expression of
674 distinct maternal and somatic 5.8S, 18S, and 28S rRNA types during zebrafish development.
675 *RNA* 2017; **23**: 1188–1199.
676 60. Hurst GDD. Extended genomes: symbiosis and evolution. *Interface Focus* 2017; **7**: 20170001.
677 61. Lagesen K, Hallin PF, Rødland E, Stærfeldt HH, Rognes T, Ussery DW. RNammer: consistent
678 annotation of rRNA genes in genomic sequences. *Nucleic Acids Res* 2007; **35**: 3100–3108.
679 62. Katoh K, Standley DM. MAFFT multiple sequence alignment software version 7: improvements
680 in performance and usability. *Mol Biol Evol* 2013; **30**: 772–780.
681 63. Huson DH, Bryant D. Application of phylogenetic networks in evolutionary studies. *Mol Biol*
682 *Evol* 2006; **23**: 254–267.
683 64. Nguyen L-T, Schmidt HA, von Haeseler A, Minh BQ. IQ-TREE: a fast and effective stochastic
684 algorithm for estimating maximum-likelihood phylogenies. *Mol Biol Evol* 2015; **32**: 268–274.
685 65. Reuter JS, Mathews DH. RNAstructure: software for RNA secondary structure prediction and
686 analysis. *BMC Bioinformatics* 2010; **11**: 129.
687 66. Nakagawa T, Kaku H, Shimoda Y, Sugiyama A, Shimamura M, Takanashi K, et al. From
688 defense to symbiosis: limited alterations in the kinase domain of LysM receptor-like kinases are
689 crucial for evolution of legume-*Rhizobium* symbiosis. *Plant J* 2011; **65**: 169–180.

690

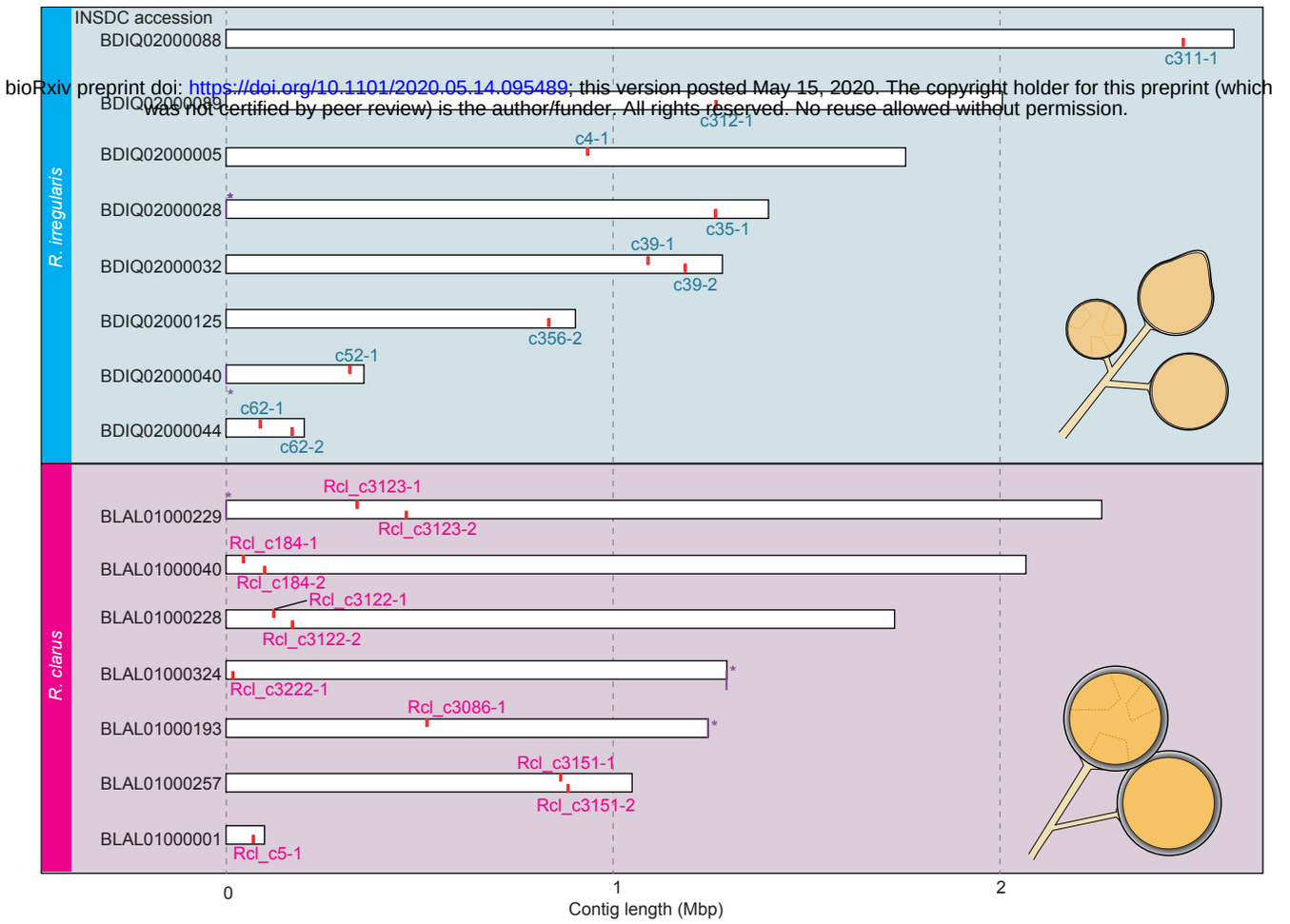

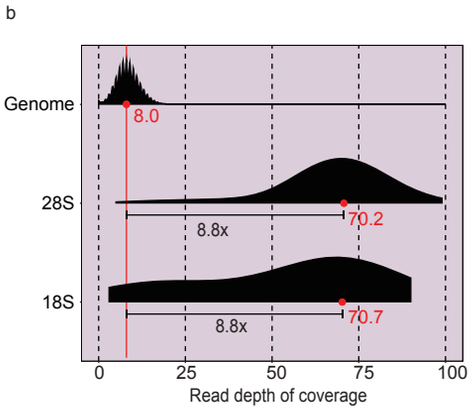

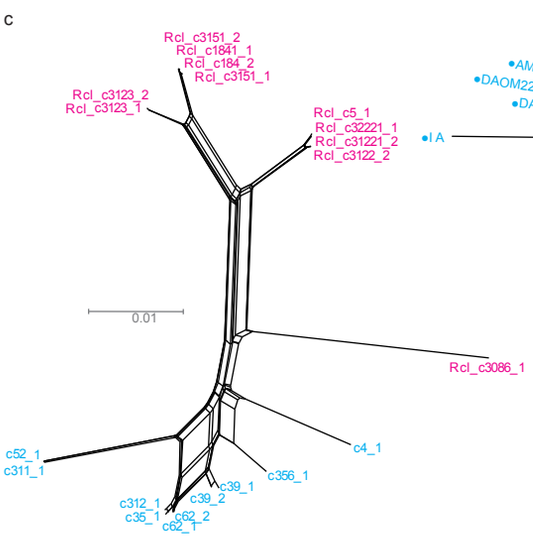

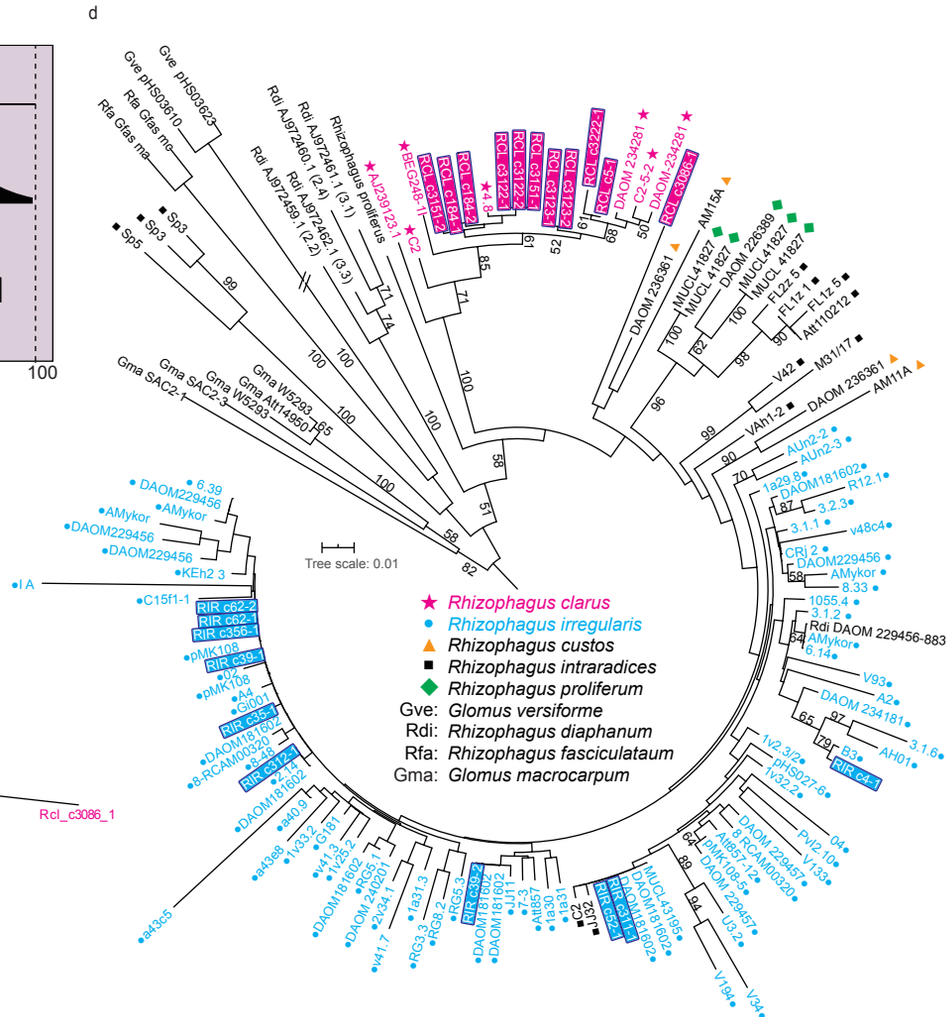

Fig. 1

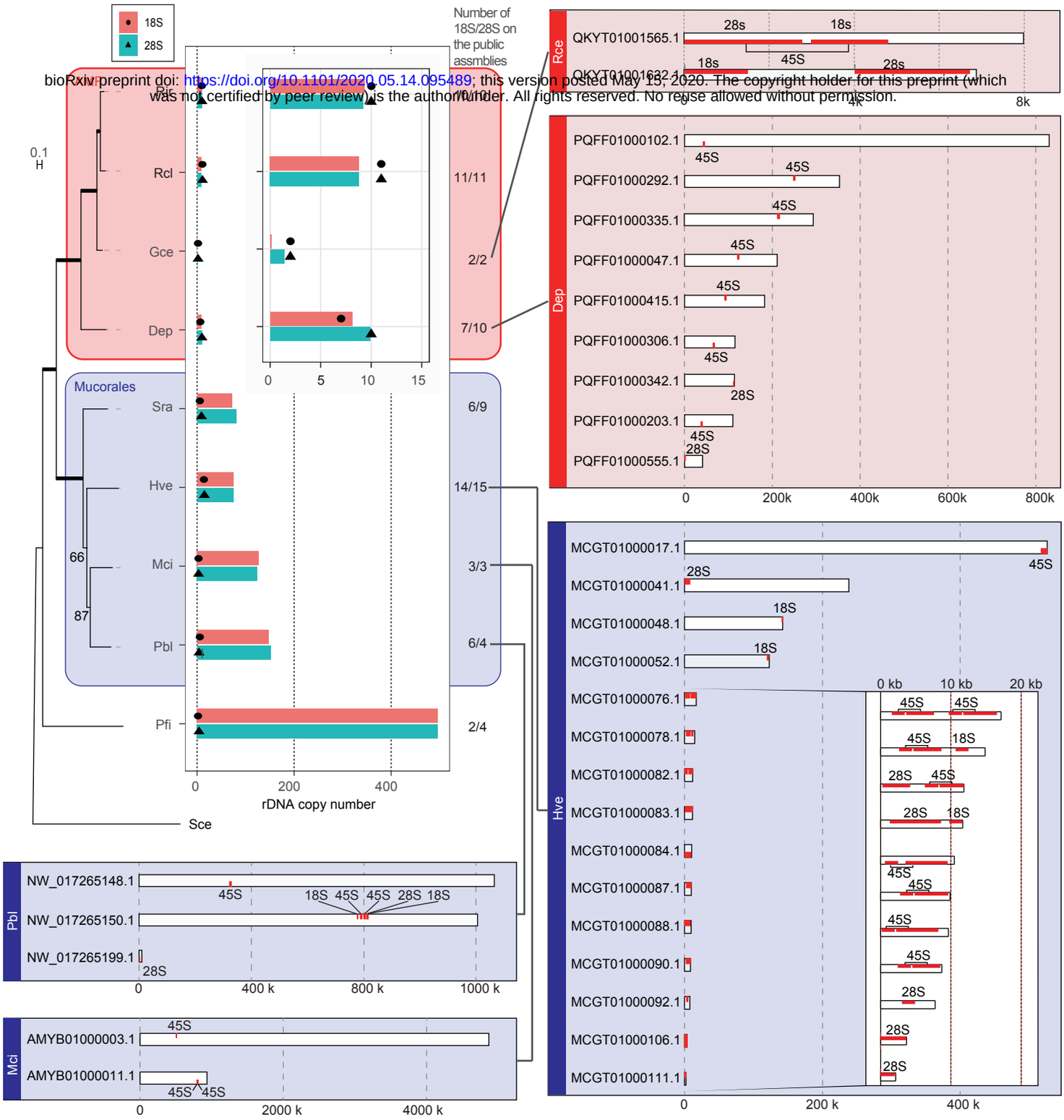

Fig. 2

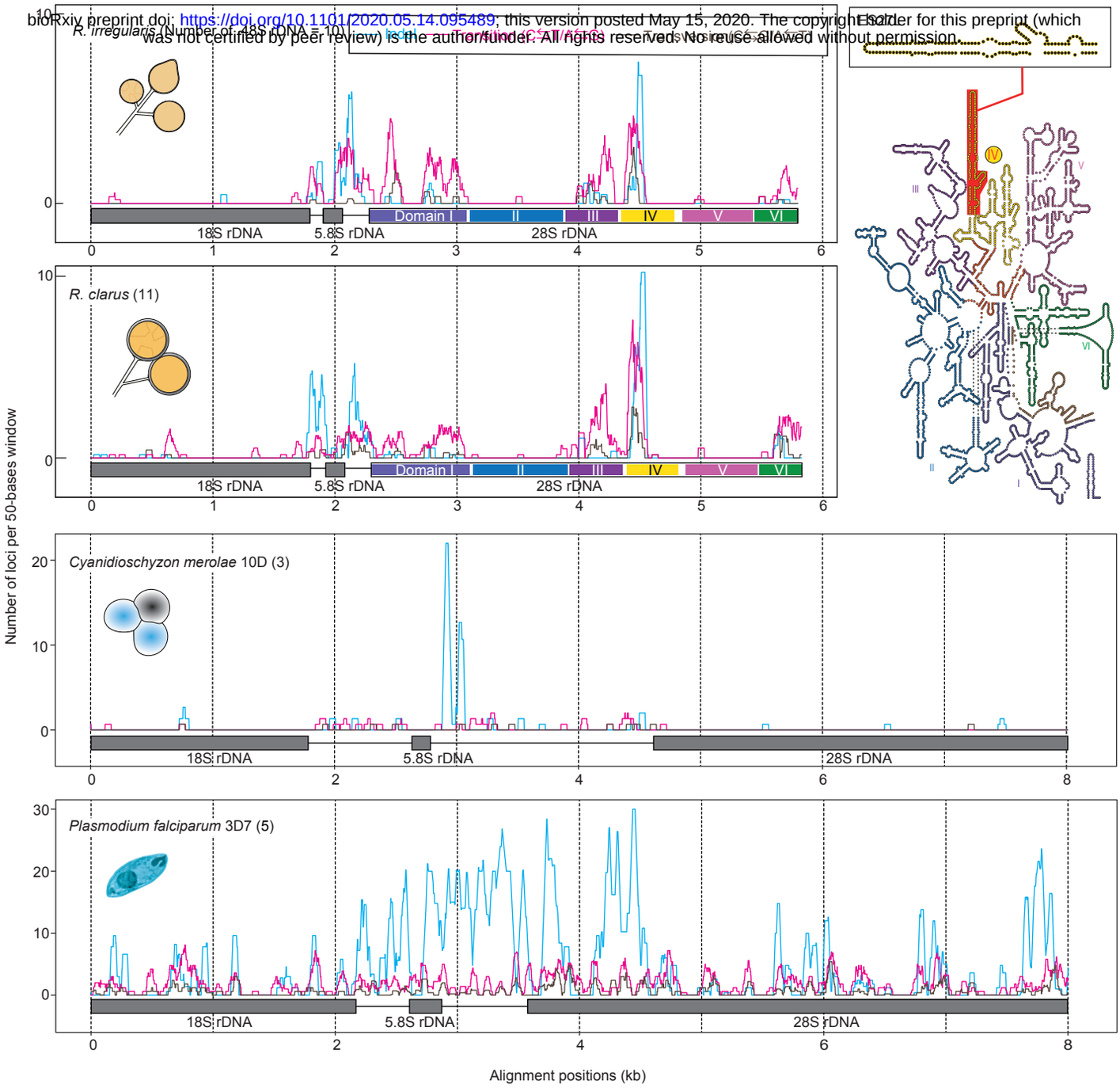

Fig. 3

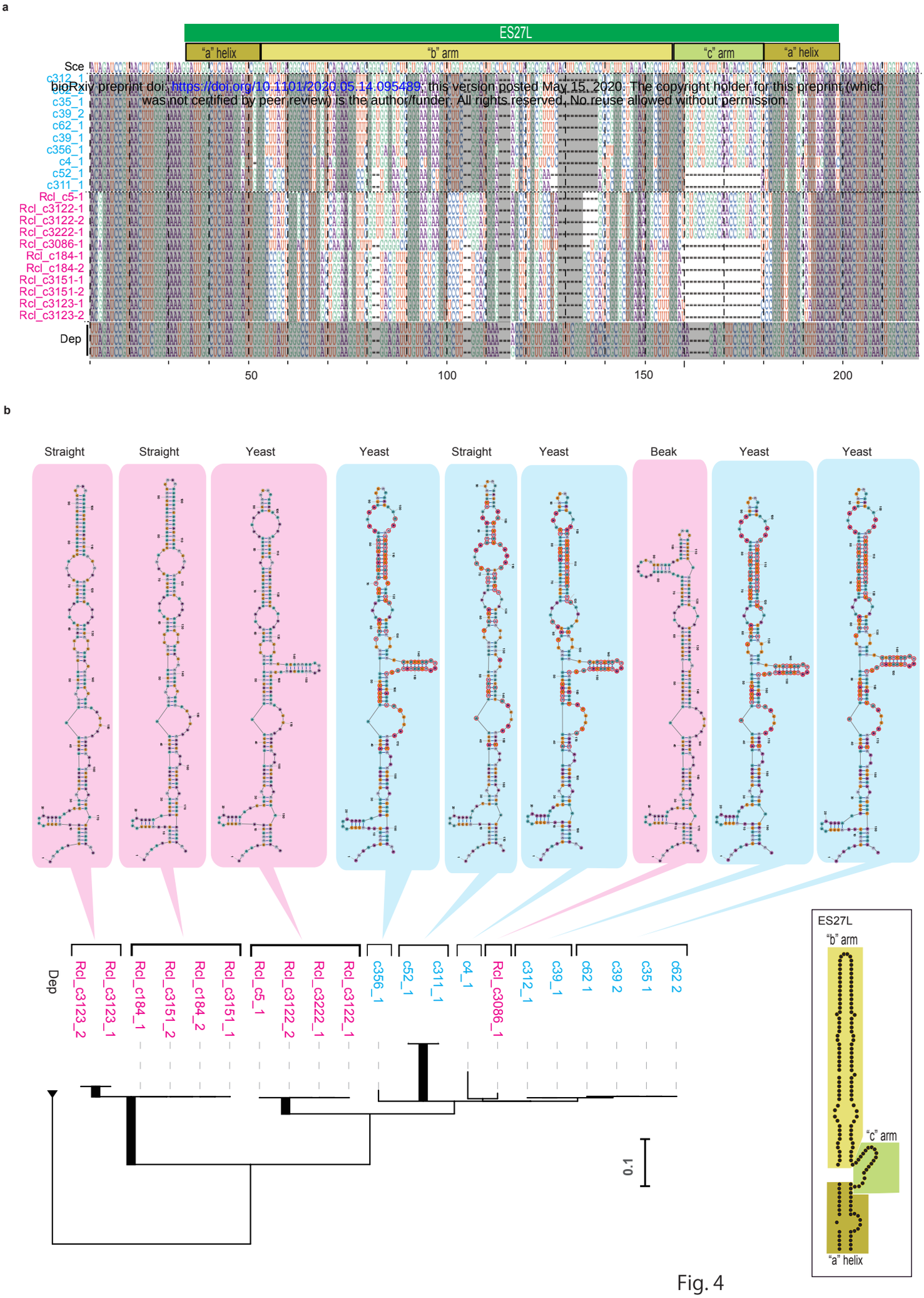

Fig. 4

A

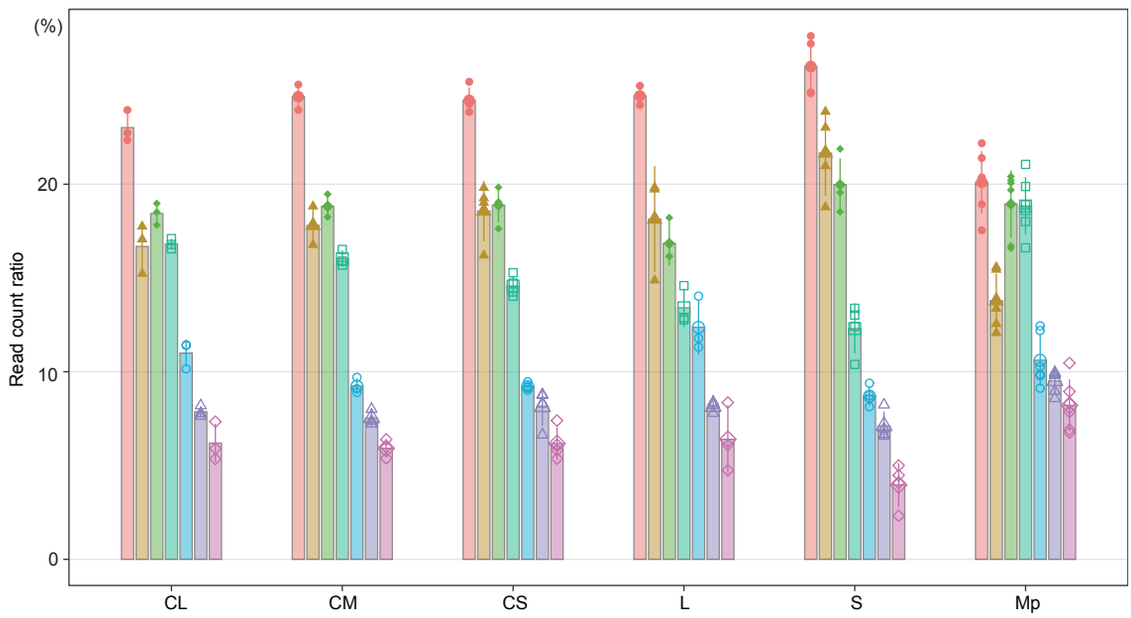

B

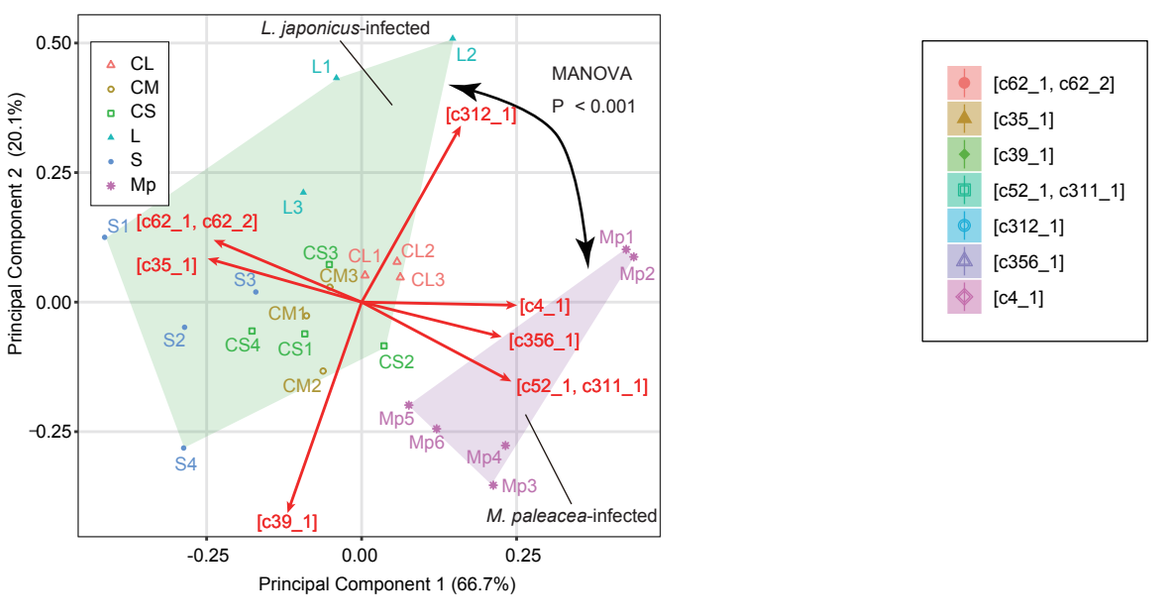

Fig. 5